Applied Computer Science, vol. 14, no. 4, pp. 34–53
doi:10.23743/acs-2018-28

Submitted: 2018-09-30
Revised: 2018-12-07
Accepted: 2018-12-16

pressure vessel, finite element, simulation, numerical analysis, tank

Paweł BAŁON [0000-0003-3136-7908]*/***, *Edward REJMAN*[**], *Bartłomiej KIEŁBASA*[*], *Janusz SZOSTAK* [0000-0002-7789-3383]***, *Robert SMUSZ* [0000-0001-7369-1162]****

NUMERICAL AND EXPERIMENTAL ANALYSIS OF THE STRENGTH OF TANKS DEDICATED TO HOT UTILITY WATER

Abstract

The focus of this paper are experimental and numerical strength tests of domestic hot water storage tanks. The tests involved the verification of the minimum wall thickness for the assumed operating parameters while meeting all safety standards. The authors presented numerical and experimental analyses for the verification of strength parameters of axial cylindrical tanks due to the lack of methodological guidelines for this type of equipment. In order to verify the conducted theoretical considerations and calculations, experimental tests of samples of front welds produced with austenitic steel as well as a pressure test for the whole tank were conducted using a research test stand.

[*] SZEL-TECH Szeliga Grzegorz, Wojska Polskiego Street 3, 39-300 Mielec, Poland, e-mail: p.balon@szel-tech.pl, e-mail: bartek.kielbasa@gmail.com
[**] Rzeszów University of Technology, The Faculty of Mechanical Engineering and Aeronautics, Department of Mechanical Engineering, Powstańców Warszawy Avenue 9, 35-959 Rzeszów, Poland, e-mail: erejman@prz.edu.pl
[***] AGH University of Science and Technology, Faculty of Mechanical Engineering and Robotics, Department of Manufacturing Systems, Mickiewicza Avenue 30-B4, 30-059 Kraków, Poland, e-mail: szostak@imir.agh.edu.pl
[****] Rzeszów University of Technology, The Faculty of Mechanical Engineering and Aeronautics, Department of Thermodynamics, Powstańców Warszawy Avenue 9, 35-959 Rzeszów, Poland, e-mail:robsmusz@prz.edu.pl

1. INTRODUCTION

A pressure vessel is a reservoir manufactured to contain fluid (liquid or gas) at a pressure substantially different from the ambient. Cylindrical pressure vessels have widespread industrial applications and have become a type of equipment widely used in industry and everyday life. They are used in power plants, nuclear reactors, chemical processing reactors, and food industries. They appear in industrial compressed air receivers and domestic hot water storage tanks. Other application areas of pressure vessels are recompression chambers, distillation towers, autoclaves, oil refineries, petrochemical plants, vehicle airbrake reservoirs, and storage tanks for liquefied gases such as ammonia, propane, butane, and LPG, etc. They often perform under extreme pressure and temperature conditions (Li, Sheng & Zhang, 2012; Lakshmi Devi & Hari Shankar, 2016). Fundamental loads acting in the tanks are internal hydrostatic pressure and internal uniform pressure. The design of the pressure vessels is mainly related to their strength and the strength study mainly includes stress concentration analysis in the neighborhood of the head and cylindrical shell joint and in the heads of the tank. Pressure vessels can be closed at the ends by different shapes of the heads from flat plates to hemispherical domes. At the junction between a cylindrical shell and a vessel head there is discontinuity of meridional curvatures. These discontinuities of curvatures disturb the membrane stress state and have significant influence on the strength of the structure. This issue has been analyzed in books (Ziółko, 1986; Harvey, 2000) and standards (PN-EN 1993-1-6:2007, 2007; PN-EN 1993-4-2:2009, 2009). One of the most important topics in design is optimal shaping of the entire structure of the tanks. In many works the problem of the optimal tank shape was analyzed (Ventsel & Krauthammer, 2001; Błachut & Magnucki, 2008; Lewiński & Magnucki, 2010, 2012) and special attention was paid to the junction between the vessel and its head because this region is usually subject to considerable stress concentration due to the edge effect (Krużelecki & Proszowski, 2012).

The aim of this work was to describe the strength performance of a cylindrical vertical domestic hot water storage tank. Numerical calculations and experimental strength tests were made to verify the wall thickness for assumed work parameters while meeting all safety standards.

The correct assessment of strength properties requires both numerical and experimental testing of the tank, including its critical nodes, e.g. welded joints. In the first stage of strength tests, tensile tests of samples, tests of mechanical parameters of material and tests of welded joints were conducted. Then an analytical estimation of peripheral and radial stress values was carried out. In the second stage, numerical analysis of the model's real object mapping was performed using the MES software. In the third stage, in order to assess the strength of the structure, strain measurements were done in the shell of the tank subjected to pressure.

The main purpose of the experimental tests was to obtain the data to assess the strength of the tank subjected to the internal pressure load. Assessment of strength

properties requires experimental tests of both: tank and critical nodes, e.g. welded joints. In the first stage of strength tests, tensile tests of welded butt joints were carried out. In the second stage the structural behavior of a cylindrical tank subjected to internal pressure was investigated.

2. TESTS OF MECHANICAL PROPERTIES OF SHEET USED ON VESSELS

2.1. Determination of the normal anisotropy coefficient R

A vessel is a device that consists of two main parts: the bottoms and the shell. While the shaping of the shell does not cause any technological problems, forming the bottoms is a serious problem. This is particularly important when shaping products with large diameters requiring expensive and heavy dies (Bałon & Świątoniowski, 2016a, 2016b; Bałon, Świątoniowski, Szostak & Kiełbasa, 2016). For this reason, the properties of the sheet material must be very precisely defined for the description of the stamping process. One of the most important parameters is the normal anisotropy coefficient R. Therefore, research on this parameter has been carried out.

The normal anisotropy R ratio by Lankford is defined as the ratio of transverse strain increments during uniaxial stretching. Assigning the main directions for flat stress state of indices: 1 – direction of rolling, 2 – direction perpendicular to the rolling direction in the plate plane, 3 – normal direction to the plate surface and determied by de_{ij} the tensor components of the plastic strain increment, this coefficient – for the sample cut at an angle α to the direction of rolling – which we can express in the form of a quotient (Bałon & Świątoniowski, 2016a, 2016b; Bałon & Świątoniowski, 2013).

$$R_\alpha = \frac{de_{22}}{de_{33}} \tag{1}$$

and respectively:

$$R_0 = \frac{de_{22}}{de_{22}} \text{ and } R_{90} = \frac{de_{11}}{de_{33}} \tag{2}$$

In practice, with homogeneous and proportional deformations, in determining the anisotropy coefficients, in the place of de_{ij} increments, the final values of real strains can be used, so the final formula will take the form (Dyrektywa 97/23/WE, 1997; Rozporządzenie Rady Ministrów, 2002):

$$R_\alpha = \frac{ln\frac{b_1}{b_0}}{ln\frac{g_1}{g_0}} \quad (3)$$

where: b_0, b_1 – widths of the sample before and after deformation,
g_0, g_1 – thicknesses of the sample before and after deformation.

The measurement results allow us to state that the value of the steel yield point determined at 100 °C with a disproportionate elongation $R_{p0,2}$ [MPa] varies from 276.1 MPa (for the 0° direction samples) to 283.5 MPa (for the 90° direction samples), which indicates no significant influence of the directivity of the material structure on its properties after rolling. This is also confirmed by the results relating to the value of immediate tensile strength R_m – 548.8 MPa (for the 0° direction samples) and 551.3 MPa (for the 90° direction samples). In turn, the damage elongation measured after assembling both parts of the sample reaches 53%.

Measurements of the strains of the samples during thier uniaxial stretching were used to determine the normal anisotropy coefficient R. The mean R_{sr} value was calculated using the dependence:

$$R_{sr} = \frac{1}{4}(R_0 + 2R_{45} + R_{90}) \quad (4)$$

where: R_0, R_{45}, R_{90} – values of normal anisotropy coefficients for the direction according to the direction of rolling, directed at an angle of 45° and transverse to the direction of rolling

The average value of the normal anisotropy coefficient in a steel sheet of DIN 1.4541 is R_{st} = 0.9832. Therefore, the value of the anisotropy coefficient for the sample cut at an angle can be described by the formula:

$$R_\alpha = \frac{ln\frac{b_1}{b_0}}{ln\frac{l_0 g_0}{l_1 g_1}} \quad (5)$$

where: b_0, b_1 – measured lengths of the sample before and after elongation.

On the basis of the conducted tests, it was found that the tested steel sheet DIN 1.4541 does not show normal anisotropy to a degree that can significantly affect the course of the pressing process. In the most general case, during stamping of the bottom from a flat disc, in the flange zone, the material is subjected to radial tensile stresses and peripheral compressive stresses, and thus the product of main stresses fulfills the unevenness $s_{11}s_{22} < 0$.

In this case, according to the condition of metal transitioning into the plastic state of Mises-Hill,

$$s_{11}^2 - \frac{2R_0}{1+R_0} s_{11}s_{22} + \frac{R_0(1+R_{90})}{R_{90}(1+R_0)} s_{22}^2 = s_p(1) \quad (6)$$

the absolute decreases, and the necesssity for plasticizing stress values $|s_{11}|$ and $|s_{22}|$ could be expected only at $R > 1$.

The bottoming operation is a cold process, hence the deformation of the material formed in subsequent phases leads – through dislocations in the crystal lattice – to the strengthening of the blank material. This phenomenon must be taken into account when determining the process parameters.

In the macroscopic analysis, the non-linear relation between stress σ, and strain φ describes the metal strengthening curve, the form of which depends on the adopted model of strengthening – isotropic or kinematic (Bałon, Świątoniowski, Szostak & Kiełbasa, 2016, 2017; Bałon, Świątoniowski & Kiełbasa, 2017).

2.2. Isotropic hardening model

In the stamping process, the kinematic model better reflects the physical aspect of the proces than the isotropic model. In the considered case of stamping, in which the load increases continuously up to the maximum value, there is no need to take into account stress hysteresis and therefore, the sufficient accuracy is ensured by a much simpler isotropic model.

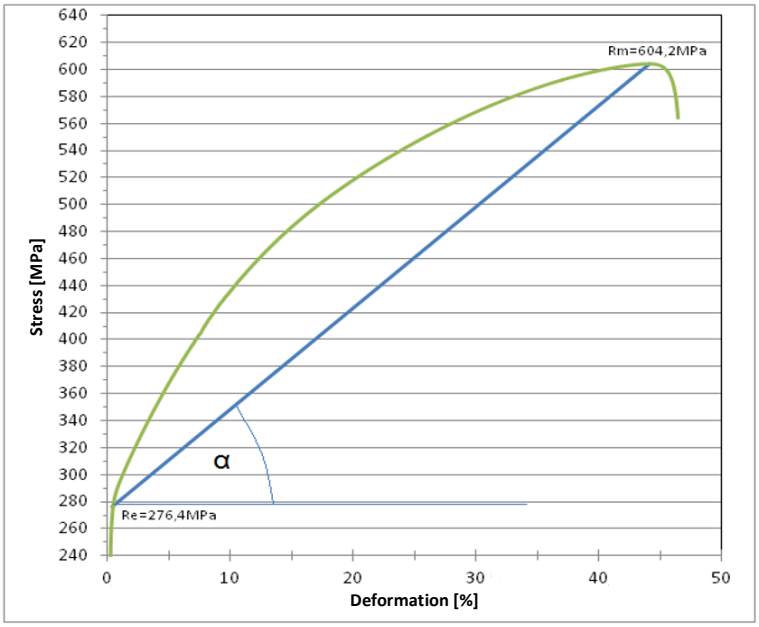

Fig. 1 Hardening curve of DIN 1.4541 steel with applied connecting section $R_{p0,2}$ and R_m (blue color) – isotropic hardening

The nonlinear material with isotropic hardening is defined by the value $R_{p0,2}$ and the value R_m, while the section between $R_{p0,2}$ and R_m is defined by the tangent of the angle of inclination of the α curve. Transformation of the stiffness matrix takes place once strain or stresse values do not exceed the value specified by $R_{p0,2}$ and above this value each time at successive iterations.

Hardening curve of the material determined with extrapolation according to the method of Krupkowsky-Gesetz:

$$\sigma_w = K * (\varphi + \varphi_0)^n \tag{7}$$

where: n = 0.31500, φ_0 = 0.00055, K = 2442.194.

3. EXPERIMENTAL RESEARCH OF FRONT WELDS

Steel 1.4541 (EN designation X6CrNiTi18-10), which was used in fabrication of the tank belongs to the largest austenitic stainless steels group with high corrosion resistance, and can be welded in all dimensions without becoming susceptible to intergranular corrosion. The chemical composition of the steel 1.4541 shown in Table 1.

Tab. 1. Chemical composition of the X6CrNiTi18-10 in %

Element	C	Si	Mn	P	S	Cr	Mo	Ni	Cu	Ti
Standard	0.08	–	2	0.045	0.015	17–10	–	12	–	0.7
Tested	0.034	–	1.20	0.021	0.001	17.21	0.057	9.12	0.10	0.394

The analysis concerns the mechanical properties of the TIG welding butt joints with argon shielding. Test samples were prepared from 2.0 mm thick sheets of steel 1.4541.

In accordance with standards, a tensile test was carried out on a certified strength machine and the results of the strength tests performed on welded joints made of steel 1.4541 under quasi-static conditions are shown in Table 2.

Tab. 2. Mechanical properties of the 1.4541 steel obtained in the tensile tests

Test No.	Ultimate tensile strength [MPa]	Average ultimate tensile strength [MPa]	Yield strength [MPa]	Average yield strength [MPa]
1	615	612.2	261	262.2
2	618		258	
3	608		269	
4	604		271	
5	616		252	

The tests show that destruction and broken areas of all samples occurred outside the heat affected zone and the tensile strength of the joint was higher than the base material. Furthermore, ultimate tensile strength (UTS) of the steel 1.4541 samples was higher than normative values of the UTS (normative UTS of the steel 1.4541: 520 MPa).

In the next step, the experimental tests on an internally pressurized tank were carried out. The subject of the experimental test was a cylindrical pressure vessel with a mean diameter of the cylindrical part equal 480 mm, made of steel X6CrNiTi18-10. The wall thickness of the cylindrical part of the tank and the top bottom head walls is the same and equal 2 mm and the main geometric dimensions of the head geometry are shown in Fig.2. The heads of the tank were manufactured by spinning and the shape of the top and middle surface of the head was defined by spline curve. The bottoms were manufactured according to the DIN 28013 norm (Warunki Urzędu Dozoru Technicznego WUDT/UC/2003, 2005; Bałon, Świątoniowski, Szostak & Kiełbasa, 2016).

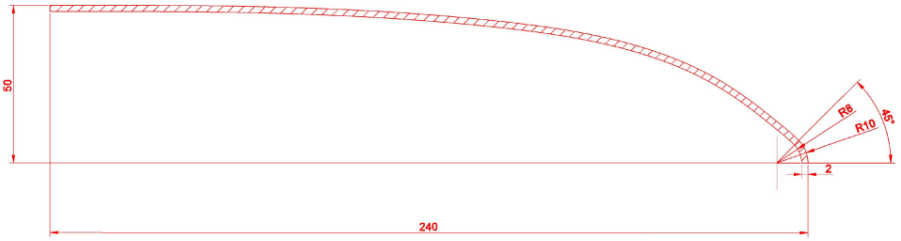

Fig. 2. Head tank geometry

For the joining of samples, the classic TIG method and the method with argon bluing on the side of the root of the weld were used. In the case of stretching samples made of X6CrNiTi18-1 steel made with the TIG method without argon bluing from the side of the ridge, the sample was destroyed in the cross-section of the weld, and for welding with the bluing – outside the weld area (Bałon & Świątoniowski, 2014).

Based on the above tests, it can be concluded that, with regard to the same welded material, the TIG welding technology using argon blown from the root side of the weld significantly improves the quality of the weld surface as well as its tensile strength. The average value of tensile strength of the connection was R_m = 630.6 MPa.

For this reason, the TIG method was proposed for the welding of the vessel, with argon bluing on the ridge side (Bałon, Świątoniowski & Szostak, 2015; Bałon & Świątoniowski, 2014).

Fig. 3. Welded sample after tensile test –X6CrNiTi18-1 (1.4541) steel – TIG welded sample with argon bluing on weld ridge

4. ANALYTICAL AND NUMERICAL STREGTH CALCULATION OF THE VESSEL

The designed tank is dedicated to storing water with a temperature of up to 100 °C and a working pressure P_1 = 6 bar equal to the pressure of water feeding from the network. Nominal, design and trial pressures were adopted in accordance with the regulatory literature in force in the European Union and Poland.

The basis for the design of the tanks is P_s pressure which is the maximum allowable pressure specified by the producer for which the device has been designed (Dyrektywa 97/23/WE, 1997; Rozporządzenie Ministra Gospodarki, 2005; PN-EN 13445-1, 2014; PN-EN 13445-3, 2014).

The following assumptions were made for the calculation of the vessel:

- V = 192 dcm^3 – volume of water in the vessel,
- P_1 = 6 bar – water pressure in the vessel corresponding to the supply pressure (working pressure),
- T_o = 10 °C = 277 °K – minimum water temperature,
- T = 70 °C = 343 °K – maximum water temperature.

Taking into account fluctuations in the water pressure in the network and the tolerance of pressure regulation in safety valves, P_S = 7.5 bar was assumed:

Hydrostatic fluid pressure:

- H = 1.1 m – the height of the liquid column,
- ρ_w = 1000 kg/m^3 – water density.

Hydrostatic pressure:

$$P_h = H * \rho_w * g = 1.1 * 1000 * 9.81 = 1.079 * 10^4\ P \tag{8}$$

Due to the negligibly low hydrostatic pressure, which is approx. 1.8% of the working pressure, its influence on the design pressure was not taken into account.

Design pressure (PN-EN 13445-1, 2014):

Base on (PN-EN 10131:2006, 2006), the design pressure P_d should meet the condition:

$$P_d = 1.5\, P_S = 11.25\ bar \tag{9}$$

Test pressure:

The test pressure P_{test} should be:

$$P_{test} = 1.43\, P_S = 10.72\ bar \tag{10}$$

The higher pressure from P_d and P_{test}: should be taken as the design pressure:

$$P_d = 11.25\ bar \tag{11}$$

For the assumed bottom geometry and pressure of P_d = 11.25 bar, numerical calculations of the bottom using the COMSOL program were performed. The maximum reduced stresses reached the value of 210 MPa, which is lower than the material yield point of about 260 MPa, so the structure is safe.

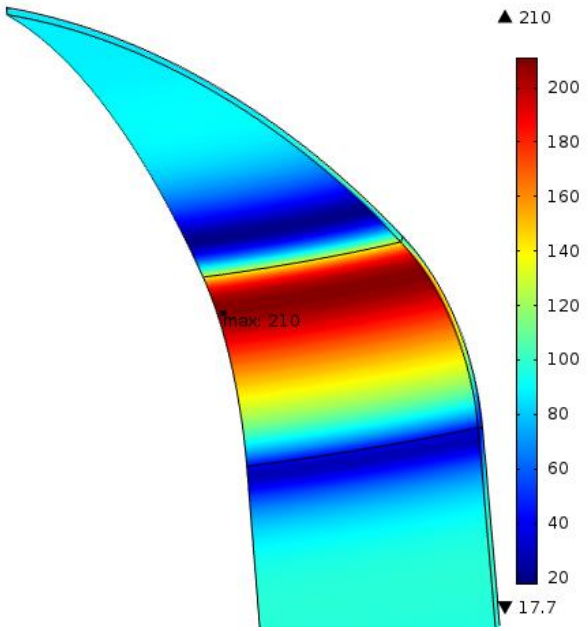

Fig. 4. A state of reduced stresses in the bottom according to DIN 28013 loaded with the design pressure of P_d = 11.25 bar, e = 2 mm – thickness of the wall (COSMOL)

In the case of vessel design according to (Rozporządzenie Ministra Gospodarki, Pracy i Polityki Społecznej, 2003), it is necessary to determine the design temperature *T*, which affects the strength properties of the vessel material. It is determined with dependencies:

$$T = T_C + 20°C \tag{12}$$

where: T_C – maximum temperature of the medium.

$$T = 70°C + 20°C = 90°C \tag{13}$$

According to (PN-EN 13445-1, 2014), the permissible stress f_d is the criterion stress for assessing the force of the vessel material. Using the design method consistent with the recognized engineering practice, and having the material from which the vessel will be made, in accordance with EN 10088-3: 2005, the strength properties of the tank material were adopted as follows:

$$R_{p1,0} = 260\ MPa \tag{14}$$

$$R_M = 540\ MPa \tag{15}$$

$$A_{min} = 35\% \text{ – elongation} \tag{16}$$

It should be stated that the material parameters obtained during the tests significantly exceed the values given by the standard. Due to the fact that the designed tank works at a temperature of T = 70 °C, it can be estimated on the basis of the EN 10088 norm that the appropriate mechanical properties for the tested steel are:

$$R_{p1,0/T} = 273\ MPa \tag{17}$$

$$R_{M/T} = 575\ MPa \tag{18}$$

The permissible stresses f_d are determined on the basis of chapter 6.4 according to (PN-EN 1993-1-6:2007, 2007).

$$f_d = \max\left[\left(\frac{\frac{R_{p1,0}}{T}}{1{,}5}\right); \min\left(\frac{\frac{R_{p1,0}}{T}}{1{,}2}\right); \left(\frac{\frac{R_m}{T}}{3}\right)\right. \tag{19}$$

$$f_d = \max[(145{,}3); \min(181{,}7)\,; (165)] \tag{20}$$

$$f_d = 165\ MPa \tag{21}$$

The *f* stresses in the structure should satisfy the following conditio:

$$f \leq f_d \tag{22}$$

4.1. Calculation of cylinder wall thickness of a tank part according to peripheral stresses

$$e = \frac{P*D_i}{2*f*z-P} \tag{23}$$

or

$$e = \frac{P*D_e}{2*f*z+P} \tag{24}$$

where: $P = P_d = 11.25$ MPa – design pressure,
e – required wall thickness,
z – connector factor (Dyrektywa 97/23/WE, 1997):
$z = 1$ – when the tested object together with the weld is subjected to destructive and non-destructive tests,
$z = 0.85$ – when the object with the weld is subjected to random non-destructive tests,
$z = 0.7$ – for non-destructive visual tests.

Considering that the assessment of weld properties was done by testing a welded metal sample and ther are conditions for visual assessment of the weld in the structure, $z = 0.85$ was accepted for the calculations.

For the internal diameter of the tank of D_e = 480 mm, the theoretical wall thickness of the tank was determined as follows:

$$e = \frac{1{,}125\frac{N}{mm^2}*480mm}{2*165\frac{N}{mm^2}*0{,}85=1{,}125\frac{N}{mm^2}} = 1.920\ mm \tag{25}$$

4.2. Calculation of the tank wall thickness with regard to operating conditions

The nominal sheet thickness e_n is determined by the formula:

$$e_n = e + C + \delta_e + \delta_m \tag{26}$$

where: C – corrosion allowance,
δ_e – allowance for tolerances of rolled sheets (lower tolerance deviation),
δ_m – wall thickness allowance due to additional pressure stresses ($\delta_m = 0$) was assumed.

According to American data for the X6CrNiTi18-1 steel (marking according to AISI – 304), the reduction in wall thickness for a working water environment for a year is (with research being carried out for 15 years):

$$C_0 = 0.0074\ \mu m/year \tag{27}$$

Assuming τ = 15 years as the expected tank life, the following was obtained:

$$C = C_0 * \tau = 0.0074 * 15 = 0{,}025\ \mu m \tag{28}$$

δ_e = 0.14 mm according to EN10131:2006 (29)

$$e_n = 1.92 + 0{,}14 + 0.00111 = 2.061\ mm \tag{30}$$

Due to the fact that the axial stresses are twice as small, the wall thickness considered in the axial direction will be smaller. The proposed solution assumes the thickness of the sheet as e_n = 2 mm.

For the proposed solution, the main stresses will be:

$$f_1 = \frac{P_d * D_m}{2 * e_n} = \frac{1{,}125 \frac{N}{mm^2} * 477{,}5\ mm}{2 * 2{,}5\ mm} = 106{,}43 \frac{N}{mm^2} = 106.43\ MPa \tag{31}$$

where: D_m – the average vessel diameter

$$f_2 = \frac{P_d * D_m}{4 * e_n} = 53.22\ MPa \tag{32}$$

$$f_{\text{rezdb}} = \sqrt{f_1^2 + f_2^2 - f_1 - f_2} = \sqrt{106{,}43^2 + 53{,}22^2 - 106{,}43 * 53{,}22} = 92.17\ MPa \tag{33}$$

According to (PN-EN 13445-1, 2014), the reduced stress should meet the condition:

$$f_{red} = \leq min\{\frac{5}{6}R_{P/T}; \frac{1}{3}R_{M/T}\} \quad (34)$$

$$\frac{5}{6}R_{P/T} = \frac{5}{6} * 218 - 181{,}7\ MPa \quad (35)$$

$$\frac{1}{3}R_{M/T} = \frac{1}{3} * 495 = 165\ MPa \quad (36)$$

$$f_{rezdb} = 92.17\ MPa < 181.7\ MPa \text{ (the condition is met)} \quad (37)$$

Taking into account that the lowest acceptable stress value, which is significantly lower than experimentally determined, was used for calculations, the sheet thickness of e = 2 mm can be considered as sufficient.

5. EXPERIMENTAL RESEARCH

The main goal of the research was to obtain the data needed for the experimental assessment of the force of the vessel material at a certain value of its internal pressure load. The object undergoing testing was a pressure vessel with an average diameter of the cylindrical part of D_{sr} = 480 mm, made of X6CrNiTi18-10 steel. The thickness of the bottom walls and the cylinder itself is the same and equals 2 mm.

Fig. 5. The view of the vessel prepared for research

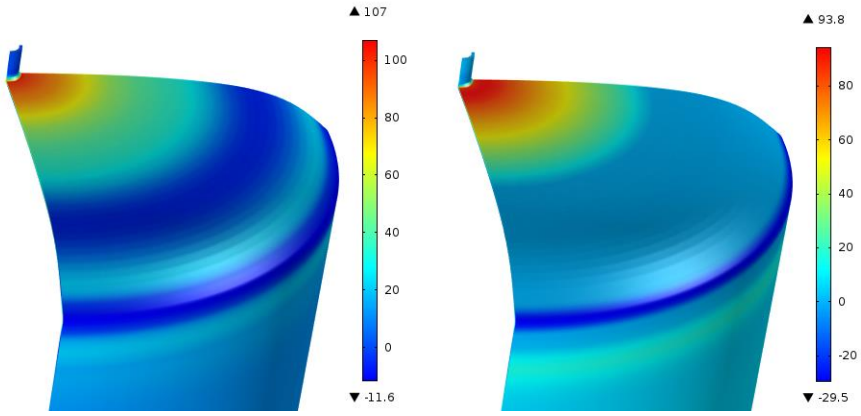

Fig. 6. Distribution of stresses in the bottom at a pressure of 0.3 MPa: circumferential stresses (left view) and radial stresses (right view)

Bottoms of cylindrical tanks usually have ellipsoidal or toroidal-spherical shapes and are characterized by their connection to the cylindrical surface of the tank in the axial plane of the cross-section at the place of the greatest curvature. This results in the disturbance of the membrane state of internal forces in the structure (Fig. 6). There is transverse force and a bending moment which cause changes in stress distribution, both in the bottom part and in the cylindrical part of the tank. Therefore, in order to select the most intensive areas of the tank, auxiliary calculations were made using the finite element method (Fig. 6).

The greatest stresses, both circumferential and longitudinal, occur in the region at the very bottom of the bottom. Then longitudinal stresses decrease, reaching negative values near the bottom connection with the cylindrical part. The circumferential stresses reach the second local maximum near the connection to the cylindrical part.

In order to determine the stresses at the characteristic points of the structure, strain gauges were glued on them. Figure 7 shows the location of the strain gauges on the bottom. For circumferential and longitudinal strain measurements, biaxial tensiometers of the type TF 3-2x / 120 from Tenmex were used.

Additionally, two strain gauges were installed on the cylindrical part. One was installed at a distance of 10 mm from the weld, and the second halfway up the cylindrical part of the tank. In addition, in order to verify the measurements, in the same configuration as for the top end, strain gauges were installed on the very bottom of the bottom. In order to compensate for the influence of temperature on the measurement results, strain gauges were mounted on the unloaded part of the tank.

For circumferential and longitudinal strain measurements, seven biaxial tensiometers of the type TF 3-2x / 120 from Tenmex were glued on to the head of the tank. In order to compensate for the influence of temperature on the unloaded steel X6CrNiTi18-10 plate single-axis strain gauges were mounted. Additionally, two

strain gauges were installed on the cylindrical part. To measure the pressure in the tank, a piezoelectric transducer was used. The strain gauges and pressure transducer were integrated with the Catman measuring system using the four Hotminger Spider-8 amplifiers. During the test, data from 26 measurement channels were recorded. The pressure test was carried out as follows. After calibrating the measurement channels and stabilizing the indications of the strain gauges, the appropriate pressure in the tank was developed by the water pump.

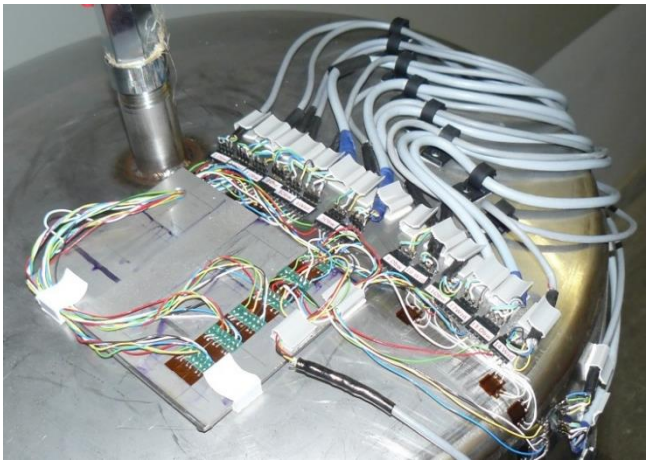

Fig. 7. View of tested tank with strain gauges

5.1. Pressure test

The pressure test was carried out as follows. After calibrating the measurement channels and stabilizing the indications from the strain gauges, the appropriate pressure value in the tank was forced by means of the pump and its constant value was maintained so as to obtain the determined conditions. This state was maintained for 15 seconds to be able to register a sufficiently large sample of measurement data. The measurement data was recorded and saved every 20 ms. At the same time, the tightness of the system was controlled, i.e., checks were made for the presence of water leaks. The pressure was measured in increments of 1 bar. The tests were carried out at a constant temperature of 24 °C.

In the pressure range from 1 to 9 bar, there was no slow pressure drop when pumping stopped. However, for higher pressures, its slow decline was noticeable, despite the pump's cessation. No leakage of water from the installation was found during this time. The pressure drop was caused by exceeding the yield point in the zone with the highest stresses, which caused the start of the “flow” of the material and the increase of the volume of the tank. This process deepened with increasing pressure, i.e. the gradient of pressure drop increased with increasing pressure level. This meant that an ever-larger material zone reached the limit of plasticity.

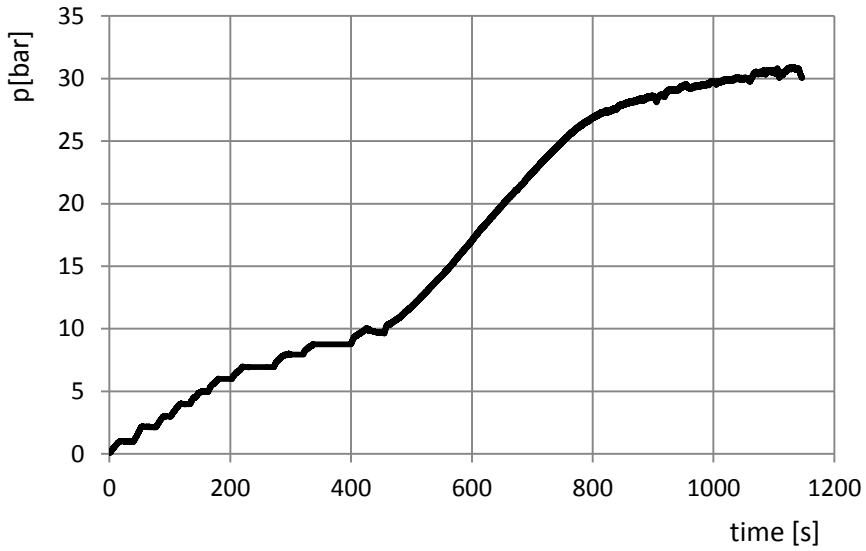

Fig. 8. Maximum pressure in the tank

The pressure test was carried out up to 30.9 bar. A further increase in pressure was not possible due to insufficient pump capacity, i.e. the plastic flow phenomenon was already so intense that it was not possible to achieve higher pressure values.

At the conclusion of the test, the tank was inspected and no leaks were found. All welded connections had been leak-proof and were undamaged.

Fig. 9. Changes in the shape of the tank bottom at an increase of pressure up to 30 bar

The degree of deformation, which is the effect of plastic deformation can be noticed by comparing the shape of the bottoms before and after the pressure test (Fig. 9).

5.2. Results of extensometer measurements

During the measurements, circumferential and longitudinal deformations were recorded, which in this case are the main deformations:

$$\epsilon_1 = \frac{1}{E} \cdot (\sigma_1 - \nu \cdot \sigma_2) \tag{38}$$

$$\epsilon_2 = \frac{1}{E} \cdot (\sigma_2 - \nu \cdot \sigma_1) \tag{39}$$

where: E – Young's modulus, ν – Poisson's ratio

In addition, dependencies are correct for the cylindrical part, based on membrane theory of coatings:

$$\sigma_1 = \frac{p \cdot D_{śr}}{2 \cdot e} \tag{40}$$

$$\sigma_2 = \frac{p \cdot D_{śr}}{4 \cdot e} \tag{41}$$

where: $D_{śr}$ – average diameter of the cylindrical part of the tank,
e – wall thickness.

Based on the above relationships and all of the following are measured: deformations, pressure, wall thickness and average tank diameter, it is possible to estimate the Young's modulus of elasticity and the Poisson's coefficient from the equations:

$$\epsilon_1 = p \cdot \frac{D_{śr}}{2e \cdot E} \cdot \left(1 - \frac{\nu}{2}\right) \tag{42}$$

$$\epsilon_2 = p \cdot \frac{D_{śr}}{2e \cdot E} \cdot \left(\frac{1}{2} - \nu\right) \tag{43}$$

The deformations ε_1 and ε_2 are linear functions of pressure. By specifying the directional coefficient of the functions (42) and (43), the Young's modulus and the Poisson's ratio values can be determined. The deformations ε_1 and ε_2 were recorded from the measurement point located on the cylindrical part of the tank, for averaged pressure values.

By approximating the measured measurement data ε_1 and ε_2 with linear functions in the pressure range 1 bar-6 bar, the directional coefficients, equations (42) and (43) were determined, which were respectively: $7.1077 \cdot 10^{-4}\ 1/MPa$ and $2.1407 \cdot 10^{-4}\ 1/MPa$.

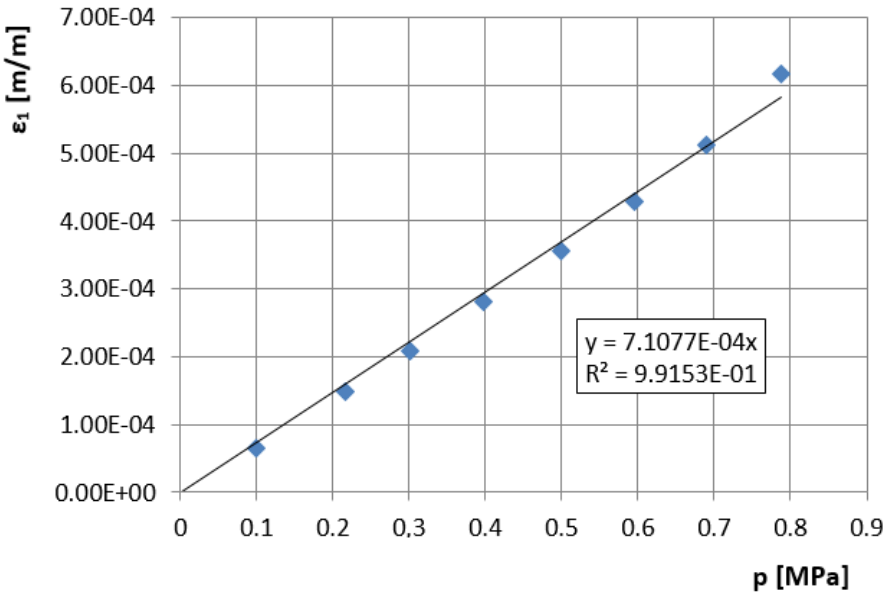

Fig. 10. Peripheral relative elongation – cylindrical part of the tank

On this basis, the Young's modulus and Poisson's ratio were estimated, the values of which were respectively: 150 GPa and 0.234.

Based on literaturę data, for the X6CrNiTi18-1 steel, Young's modulus at 20 °C ranges from 190 to 200 GPa. The Poisson's ratio varies from 0.24 to 0.3. The discrepancy between the literature data and the Young's modulus and the coefficient obtained from measurements was 23% and 13%, respectively. It is the result of measurement uncertainty of component quantities.

As can be seen, there is a linear dependence of strain at all measuring points in the pressure range from 1 to 8 bar, with the exception of point 6.

Using the determined Young's modulus and Poisson's ratio, the measured strains were transformed into stresses using the following relationships:

$$\sigma_1 = \frac{E}{1-\nu^2} \cdot (\varepsilon_1 + \nu \cdot \varepsilon_2) \tag{44}$$

$$\sigma_2 = \frac{E}{1-\nu^2} \cdot (\varepsilon_2 + \nu \cdot \varepsilon_1) \tag{45}$$

The circumferential stresses tend to decrease as the distance from the symmetry axis of the tank increases. This state maintains up to a point with a coordinate of approx. 230 mm, where the sign changes and the state of compressive stress changes.

At a distance of about 170 mm, circumferential (tensile) stresses reach the local minimum, then increase rapidly and change the sign.

The highest compressive (peripheral) stresses occur along the radius of the bottom passage into the cylindrical part. It is the effect of combining the ellipse with the straight part forming the cylindrical part of the tank. There is a transverse force and a bending moment that causes stress accumulation, both in the bottom part and in the cylindrical part of the tank.

Longitudinal stresses are positive (stretching) up to the point of 230 mm, where they change the sign. Along with the increase of the radius there is a slight decrease to the point with the coordinate of 70 mm. Then they grow again up to 220 mm, where they reach their maximum value.

As in the case of circumferential stresses, there is stress accumulation in the transition zone in the cylindrical part.

As you can see, this area has a decisive impact on the strength of the structure.

6. CONCLUSIONS

The conducted numerical and experimental studies show that the FEM method gives results inflated in relation to the analytical calculations, although it indicates the directions where the maximum stress increases should be expected.

The analytical method recommended by the relevant standards allows for the safe design of tanks and the maintenance of good safety ranges.

The material properties of steel given by standards are smaller than the actual values. When designing, for minimal safety factors, you must have your own material base, created as a result of tests in certified laboratories.

In the construction of tanks made of austenitic steel, exceeding the yield point is not synonymous with the destruction of the structure. For large stress values (exceeding the yield point) significant deformations and displacements occur, but the structure remains sealed.

Austenitic steels show good weldability, and the selection of a suitable welding technology ensures adequate weld strength and preservation of its integrity even when the parent material is destroyed.

REFERENCES

Bałon, P., & Świątoniowski, A. (2013). The influence of cold forming conception on the springback magnitude. *Key Engineering Materials*, *554–557*, 2299–2311.

Bałon, P., & Świątoniowski, A. (2014). Forming of automotive parts with nuts clinch process in comparison to welding of nuts. *Key Engineering Materials*, *611–612*, 1503–1510.

Bałon, P., & Świątoniowski, A. (2014). Stamping automotive parts with clinch nut process. *AIP Conference Proceedings*, *1567*, 971–974.

Bałon, P., & Świątoniowski, A. (2016a). Analiza procesu formowania dennicy hybrydowego urządzenia grzewczego. *Mechanik: miesięcznik naukowo-techniczny*, *12*, 1840–1843.

Bałon, P., & Świątoniowski, A. (2016b). Improved method of springback compensation in metal forming analysis. *Strength of Materials*, *48*(4), 540–550.
Bałon, P., Świątoniowski, A., & Kiełbasa, B. (2017). The analysis of bottom forming process for hybrid heating device. *AIP Conference Proceedings*, *1896*, 170001.
Bałon, P., Świątoniowski, A., & Szostak, J. (2015). Łączenie elementów struktury samochodu z zastosowaniem wtłaczania i zgrzewania części złącznych. In J.Mucha (Ed.), *Badania i kierunki rozwoju technologii połączeń przetłaczanych na zimno: konstrukcje – procesy – zastosowanie* (pp. 221-236). Rzeszow, Poland: Oficyna Wydawnicza Politechniki Rzeszowskiej.
Bałon, P., Świątoniowski, A., Szostak, J., & Kiełbasa, B. (2016). The analysis of bottom forming process for hybrid heating device. In J. Mucha (Ed.), *Progressive technologies and materials* (pp. 7–22). Rzeszów, Poland: Oficyna Wydawnicza Politechniki.
Bałon, P., Świątoniowski, A., Szostak, J., & Kiełbasa, B. (2017). Springback compensation for a vehicle's steel body panel. *AIP Conference Proceedings*, *1896*, 080001.
Błachut, J., & Magnucki, K. (2008). Strength, stability, and optimization of pressure vessels: Review of selected problems. *Applied Mechanics Reviews*, *61*(6), 1–33.
Dyrektywa 97/23/WE Parlamentu Europejskiego i Rady z dnia 27.05.1997 w sprawie zbliżenia ustawodawstwa Państw Członkowskich dotycząca urządzeń ciśnieniowych. (1997).
Harvey, J. F. (2000). *Theory and Design of Pressure Vessels*. New Delhi: CBS Publishers & Distributors.
Krużelecki, J., & Proszowski, R. (2012). Shape optimization of thin-walled pressure vessel end closures. *Structural and Multidisciplinary Optimization*, *46*, 739–754.
Lakshmi Devi, E., & Hari Shankar, V. (2016). Modeling and Analysis of Cryogenic Pressure vessel using FEA. *International Journal of Engineering Trends and Technology (IJETT)*, *42*, (5), 261–265.
Lewiński, J., & Magnucki, K. (2010). Shaping of a middle surface of a dished head of a circular cylindrical pressure vessel. *Journal of Theoretical and Applied Mechanics*, *48*(2), 297–307.
Lewiński, J., & Magnucki, K. (2012). Optimal shaping of middle surface of a dished head of circular cylindrical vessel with the help of B´ezier curve. *ASME 2010 Pressure Vessels and Piping Conference*, *5*, PVP2010-25208.
Li, J., Sheng, J., & Zhang, Y. (2012). Simulation Research of a type of Pressure Vessel under Complex Loading Part 2 Complex Load of the Numerical Analysis. *Advances in Intelligent Systems Research*, *26*, 4114.
PN-EN 13445-1. (2014). *Nieogrzewane płomieniem zbiorniki ciśnieniowe*. Część 1: Wymagania ogólne.
PN-EN 13445-3. (2014). *Nieogrzewane płomieniem zbiorniki ciśnieniowe*. Część 3: Projektowanie.
PN-EN 1993-1-6:2007. (2007). *Design of steel structures-Strength and stability of shell structures*.
PN-EN 1993-4-2:2009. (2009). *Design of steel structures-Tanks*.
Rozporządzenie Ministra Gospodarki z dnia 21.12.2005 w sprawie zasadniczych wymagań dla urządzeń ciśnieniowych i zespołów urządzeń ciśnieniowych. (2005).
Rozporządzenie ministra Gospodarki, Pracy i Polityki Społecznej z dnia 9.07.2003 w sprawie warunków technicznych dozoru technicznego w zakresie eksploatacji niektórych urządzeń ciśnieniowych. (2003).
Rozporządzenie Rady Ministrów z dnia 16.07.2002 w sprawie rodzajów urządzeń technicznych podlegających dozorowi technicznemu. (2002).
Ventsel, E., & Krauthammer, T. (2001). *Thin Plates and Shells. Theory, Analysis and Applications*. Basel, New York, USA: Marcel Dekker Inc.
Warunki Urzędu Dozoru Technicznego WUDT/UC/2003 (2005). *Urządzenia ciśnieniowe*. Wydanie II, Warsaw.
Ziółko, J. (1986). *Metal Tanks for Liquids and Gases* (in Polish). Warsaw, Poland: Arkady.